

# HybMT: Hybrid Meta-Predictor based ML Algorithm for Fast Test Vector Generation

Shruti Pandey

Department of Electrical Engineering  
Indian Institute of Technology, Delhi  
New Delhi, India  
shruti.pandey@ee.iitd.ac.in

Jayadeva

Department of Electrical Engineering  
Indian Institute of Technology, Delhi  
New Delhi, India  
jayadeva@ee.iitd.ac.in

Smruti R. Sarangi

Department of Electrical Engineering  
Indian Institute of Technology, Delhi  
New Delhi, India  
srsarangi@cse.iitd.ac.in

**Abstract**—Testing an integrated circuit (IC) is a highly compute-intensive process. For today’s complex designs, tests for many hard-to-detect faults are typically generated using deterministic test generation (DTG) algorithms. Machine Learning (ML) is being increasingly used to increase the test coverage and decrease the overall testing time. Such proposals primarily reduce the wasted work in the classic Path Oriented Decision Making (PODEM) algorithm without compromising on the test quality. With variants of PODEM, many times there is a need to backtrack because further progress cannot be made. There is thus a need to predict the best strategy at different points in the execution of the algorithm. The novel contribution of this paper is a 2-level predictor: the top level is a meta predictor that chooses one of several predictors at the lower level. We choose the best predictor given a circuit and a target net. The accuracy of the top-level meta predictor was found to be 99%. This leads to a significantly reduced number of backtracking decisions compared to state-of-the-art ML-based and conventional solutions. As compared to a popular, state-of-the-art commercial ATPG tool, our 2-level predictor (HybMT) shows an overall reduction of 32.6% in the CPU time without compromising on the fault coverage for the EPFL benchmark circuits. HybMT also shows a speedup of 24.4% and 95.5% over the existing state-of-the-art (the baseline) while obtaining equal or better fault coverage for the ISCAS’85 and EPFL benchmark circuits, respectively.

**Index Terms**—PODEM, stuck-at-fault, ATPG, ANN, ML

## I. INTRODUCTION

VLSI testing has always been regarded as a very complex and time-intensive process. The cost of testing a single chip typically requires tens of millions of dollars, and it varies with the test time and the frequency with which the test vectors are applied to the *circuit under test* (CUT) [1]. Testing methodologies have to continuously adapt to newer fault models, especially with angstrom-era technologies.

Consider present-day automotive systems, which are big consumers of semiconductor chips. They use a wide variety of electronic components, ranging from single-transistor devices to systems-on-chip (SoCs) with billions of transistors. These automotive ICs account for 77% of customer returns in the automotive industry [2]. They control important aspects of the vehicle that were hitherto controlled manually. Hence, the defect tolerance of these automotive ICs has reduced considerably. Also, it is a well-known fact that even if the yield is very high, high fault coverage is required to achieve a near-zero defect level. To get such a low defect density, the testing

process needs to be very effective and once that is ensured, we need to work on reducing the testing time as much as possible. It is important to understand that the process of test generation and subsequent testing takes up a large fraction of the overall product conceptualization to market time. A delay of a few days can affect the product’s prospects quite negatively [3] given that it allows rivals to get an upper hand, and increases the pressure on warehouses that store partially manufactured vehicles and auto parts [4]. Hence, given the market pressures, vendors try to release a chip as soon as possible. Given the limited amount of time that they have, they need to run as many tests as possible. As a result, *keeping the coverage above a threshold, the reduction of the test generation time is of paramount importance and therefore it is our primary goal in this paper.* This is on the lines of similar recent work in this area [5]–[7].

The test engineer’s intuition and experience are typically used as heuristics to make the process manageable and quick in the case of very large circuits [8]. Human experience-based or institutional knowledge-based problem solving is both error-prone and time-consuming. It is also not a scalable solution and works to the detriment of many upstart companies. ML algorithms, on the other hand, have proven their efficacy and have been shown to be faster and more accurate in areas such as computer vision [9], natural language processing [10], and electronic design automation [11]. They provide a more level playing field in this case, as long as good quality training data can be generated.

Due to the easy availability of high-compute resources, training of large neural networks has become feasible, and hence these models are being used to automate and accelerate the various steps in the design flow. ML has been used in various stages such as lithography and mask detection [12], logic synthesis [13], IR drop prediction [14], power delivery network design [14], routing congestion prediction [15], local hotspot detection [16] and power supply noise prediction during testing [17].

Our nearest competing work [5] is a neural network that uses a single hidden layer sandwiched between two fully connected layers to solve this problem. We refer to it as the *baseline* in this paper; till date, this is the most effective model for reducing backtracking in PODEM (Path-Oriented Decision

Making) and reducing the resultant CPU time. The baseline and other prior related works have trained and evaluated their proposed neural networks on the ISCAS'85 circuits. Hence, we have also relied on the ISCAS'85 circuits to train our models. This ensures a fair comparison with the baseline. We shall compare the results of our proposed approach with the results obtained from this algorithm (taken as the baseline) on ISCAS'85 circuits to establish the performance gain of our algorithm over the baseline. We then put our proposed HybMT algorithm (trained on the smaller circuits of ISCAS'85) to test on the much more contemporary EPFL suite [18] and also compare our results with a widely used commercial ATPG tool<sup>1</sup>. It is important to note that the EPFL circuits are very large compared to the ISCAS'85 circuits. Also note that we are targeting the combinational ATPG only, hence, we do not use the sequential benchmarks (e.g., ITC'99).

Our proposed approach uses a 2-level predictor, where we use a meta predictor at the top level to choose a lower-level predictor. It is highly accurate and robust. Then we choose a variety of lower-level predictors that were chosen out of an exhaustive list of learners based on their accuracy, run times, and suitability.

Our proposed *HybMT* model shows an overall reduction of **24.4%** and **95.5%** in the CPU time on an average for the ISCAS'85 [19] and EPFL [18] benchmark circuits as compared to the baseline. We also propose a new PODEM backtracking predictor *HybNN* that is a contribution in itself. It accounts for an **18.8%** speedup in the ISCAS'85 circuits. Finally, note that *HybMT* uses random forests and decision trees, which make it explainable to a large extent. We have posted all our code and models online.<sup>2</sup>

An astute reader may argue that PODEM is a very old algorithm and so are ISCAS'85 circuits. The point that should be noted here is that all ML-based ATPG algorithms that we are aware of have been built on PODEM (albeit, highly optimized versions of it) and have been evaluated on the ISCAS'85 suite [19]. We have done the same. We use the version of the PODEM algorithm that is a part of the Fault [20] ATPG tool (part of Google's OpenLane suite); it has many built-in optimizations and is the state-of-the-art insofar as open source EDA/ATPG is concerned. In the rest of the paper, we will be using this version of the PODEM algorithm. To allay other concerns, we also compared Fault's PODEM algorithm with the other options available in Fault such as the *fanout-oriented algorithm* (FAN) [21]. PODEM outperformed them. To the best of our knowledge, our nearest competing works have not done this.

Our specific contributions are as follows:

- Modifications to the PODEM algorithm to incorporate ML-based predictions for our *no-backtrack probability*-based custom heuristic.

- Design of a novel neural network *HybNN* to serve as a backtrace heuristic in PODEM.
- Design of a novel meta-predictor that selects the best prediction model for each circuit net at runtime.
- Design and implementation of a novel 2-level predictor *HybMT* based PODEM, which is highly accurate, robust, and much faster than existing state-of-the-art approaches.
- Demonstration of significant speedup over a commercial ATPG tool and the existing state-of-the-art ML-based algorithm.

Our paper is organized as follows: Section II presents the background of the PODEM algorithm and other key concepts involved in our work. We present the methodology used in our work in Section III followed by the experiments and their results in Section IV. Next, we present the related work in Section V and finally conclude in Section VI.

## II. BACKGROUND

### A. Path Oriented Decision Making (PODEM)

Path Oriented Decision Making (PODEM) [22] is a fault-oriented deterministic test generation (DTG) algorithm that works by making assignments only at the *primary inputs* (PIs). PODEM consists of the objective, backtrace, implication, and backtrack subroutines. The *objective* subroutine is used to find the value that a net needs to be set to for the purpose of fault activation and propagation. The *backtrace* procedure involves the mapping of a desired objective to a PI and thus involves decision making at the logic gates that may have multiple inputs. It may be possible that the backtrace procedure fails to make progress and it gets stuck [23], [24]. There is thus a need to reverse some decisions and make backward progress to a point where the process of PI assignment can begin again. This procedure is known as *backtracking*. The *implication* procedure involves the logic simulation of the circuit due to a PI assignment.

### B. Design for Testability Measures

*Controllability/Observability Program (COP)*: Here, controllability [25] is defined as the probability of setting a net  $x$  to 0 or 1 by making random PI assignments (each input net has a 50% probability of being 1). *Observability* is defined as the probability of propagating the value at a net to a primary output (PO).

*Sandia Controllability/Observability Analysis Program (SCOAP)*: The SCOAP [26] combinational controllability is defined as the difficulty of setting a net's logic level to 1/0. It is represented as CC1/CC0 (resp.). It is the minimum number of PIs required to set the value of net  $x$  to a given value  $v$ . The SCOAP combinational observability is defined as the difficulty of observing the value at an internal net at a PO. It is denoted as CO. It is the minimum number of PI assignments that need to be made to propagate the fault to a PO. Note that SCOAP measures do not take reconvergent fanouts into account.

<sup>1</sup>We are working with the vendor to see if we can print the name of the tool given the no-benchmarking clause in the purchase agreement.

<sup>2</sup>The code and models are available at this anonymous link: <https://sites.google.com/view/vlsitestesting22/home>

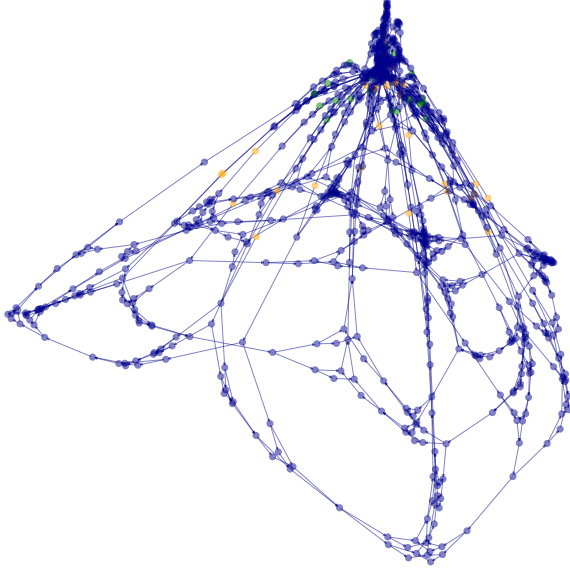


Fig. 1. Graph representation of the circuit c1908 from the ISCAS'85 benchmark

### III. METHODOLOGY

#### A. Benchmark Circuits

##### 1) ISCAS'85 Benchmark Suite of Circuits

The ISCAS'85 benchmark suite of circuits [19] is a collection of ten gate-level netlists of combinational circuits. The circuit nodes are present in a levelized order in these netlists. The gates at the PI are at level '0', then the level is incremented by one for the gates coming after that till the PO. The ISCAS'85 format has been widely used in the ATPG literature. The attributes of these circuits are shown in Table I.

TABLE I  
THE ISCAS'85 BENCHMARK CIRCUITS AND THEIR ATTRIBUTES.

Name	Function	#Total Gates	#Input Lines	#Output Lines	#Faults <sup>a</sup>
C432	Priority Decoder	160	36	7	524
C499	ECAT	202	41	32	758
C880	ALU and Control	383	60	26	942
C1355	ECAT	546	41	32	1574
C1908	ECAT	880	33	25	1879
C2670	ALU and Control	1193	233	140	2747
C3540	ALU and Control	1669	50	22	3428
C5315	ALU and Selector	2307	178	123	5350
C6288	16-bit Multiplier	2406	32	32	7744
C7552	ALU and Control	3512	207	108	7550

<sup>a</sup>Reduced equivalent fault set based on equivalence fault collapsing.

##### 2) The EPFL Combinational Benchmark Suite of Circuits

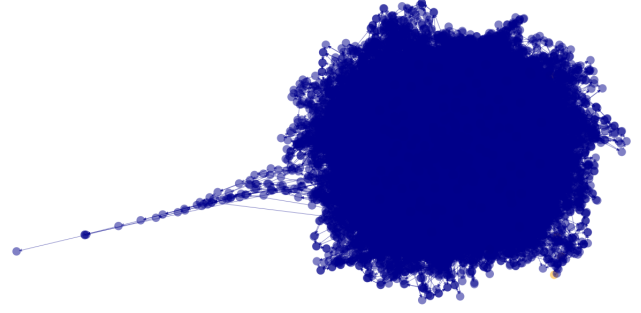


Fig. 2. Graph representation of the circuit square-root from the EPFL benchmark

The EPFL benchmark suite [18] is a more modern benchmark suite that comprises a set of arithmetic, random, and control circuits along with a few large combinational circuits (designed to test the limits of ATPG algorithms). These circuits are represented as AND/Inverter graphs. It is widely used by ATPG researchers as of today for reporting coverage numbers [27]–[29]. However, we are the first to report the CPU time of the ATPG algorithms for these circuits, to the best of our knowledge. The works in [27]–[29] target test point insertion and analysis of the impact of a circuit's structure on fault coverage, which is different from our target, i.e., minimizing the test generation time subject to a minimum coverage constraint. The EPFL benchmark circuits are much larger (at most 100 times) as compared to the ISCAS'85 benchmark circuits in terms of the total number of gates. The attributes of these circuits are shown in Table II. Our ATPG flow takes netlists in the BENCH format as input. Hence, we have taken the EPFL circuits available in the BLIF format and converted them to the BENCH format using the ABC tool [30]. Figures 1 and 2 show the graph representation of the circuits, where the vertices and edges represent the gates and their interconnections, respectively.

TABLE II  
THE EPFL BENCHMARK CIRCUITS AND THEIR ATTRIBUTES.

Name	#Inputs	#Outputs	#AND Nodes	#Levels
Adder	256	129	1020	255
Barrel shifter	135	128	3336	12
Divisor	128	128	44762	4470
Hypotenuse	256	128	214335	24801
Log2	32	32	32060	444
Max	256	130	2865	287
Multiplier	128	128	27062	274
Sine	24	25	5416	225
Square-root	128	64	24618	5058
Square	64	128	18484	250

#### B. Implementation Details

Figure 3 illustrates the decision-making involved during backtracing and the use of *no-backtrack probability* ( $p$ ) as a

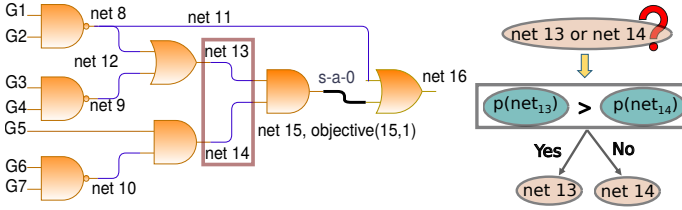


Fig. 3. Decision making during backtracing and the use of ‘probability of no-backtrack’ ( $p$ ) as a heuristic

heuristic in ML-guided PODEM. We compare the probabilities of not backtracking at both the nets (net 13 and net 14) for choosing a path during backtrace as shown in Fig. 3. Needless to say, we first choose that net that has a lower backtracking probability (as estimated by our algorithm). Next, we describe the methods used for implementing the ML-guided PODEM algorithm.

1) **Input Features of the ML Model:** The following features are given as inputs to the ML models at both the bottom and top levels of our 2-level predictor design.

- 1) *The COP Combinational Controllability:* The COP combinational controllability of a net  $l$  (represented as  $CC(l)$ ) indicates the probability of setting a net  $l$  to logic ‘1’. First, we assign the CC values for all the PIs to 0.5 as the PIs need to take the values ‘1’ and ‘0’ randomly. We use the truth tables of different gates to derive the formulae for computing the CC values for the respective output nets of these gates. Then, we calculate the CC values for the intermediate nets and POs of the circuit by traversing the circuit graph in the forward direction.
- 2) *The COP Combinational Observability:* The COP Combinational Observability of a net  $l$  (represented as  $CO(l)$ ) indicates the probability of observing the value of net  $l$  at a PO. First, we assign the CO values for all the POs to ‘1’ as any error at the POs is always observable. The formulae for computing the CO values for the input nets of different gates, given the CO values of the output net and CC values of the other input nets, are derived using the truth tables of these gates. Then, we calculate the CO values for the intermediate nets and PIs of the circuit by traversing the circuit graph in the backward direction and using the derived formulae.
- 3) *The shortest distance of a net from the PIs:* The ‘distance’ feature is normalized to bring the values in the range  $[0, 1]$  using the following formula

$$distance(l)' = \frac{distance(l) - distance_{min}}{distance_{max} - distance_{min}} \quad (1)$$

where  $distance_{min}$  and  $distance_{max}$  are the minimum and maximum values for the distance feature computed across all the circuit net samples, respectively.

- 4) *The type of the gate:* The supported gate types are PI, PO, PPI, PPO, NOT, AND, NAND, OR, NOR, XOR, XNOR, DFF, BUF and BAD. The type-of-the-gate feature is represented using 14 bits; we use one-

hot encoding. PPI and PPO stand for pseudo-primary inputs and pseudo-primary outputs, respectively, while DFF and BUF stand for D flip-flops and buffers. The gate type BAD represents gates that do not belong to any of the specified gate types.

- 5) *SCOAP zero controllability (CC0) and SCOAP one controllability (CC1):* First, we assign the CC0 and CC1 values for all the PIs to 1 and set the depth of each of the logic gates to 1. We compute the sum of the SCOAP controllability values of different input net assignments that justify the desired value at the output net. Then, we take the minimum of these sums and add it to the depth of the gate to get the CC0/CC1 value at the output of the respective logic gate. Finally, we use the CC0 and CC1 values of the logic gate outputs to figure out the CC0 and CC1 values of all the nets by going through the circuit graph in the forward direction.
- 6) *SCOAP observability (SCOAP CO):* First, we assign the CO values for all the POs to 0. Then, we compute the CO value of a logic gate’s input as the sum of the CC0/CC1 values of the other input nets, the CO value of the gate’s output net, and the depth of the gate. The lower the values of the SCOAP measures for a net, the easier it is to control and observe that net.
- 7) *Fanout of the gate:* The fanout of a gate is the number of logic gate inputs driven by the output of the logic gate under consideration.

The input features are shown in Table III.

TABLE III  
THE INPUT FEATURES FOR THE LEARNING MODELS. OUR LOWER-LEVEL PREDICTORS (ML MODELS AND HYBNN) REQUIRE THE FIRST 4 FEATURES AND HYBMT REQUIRES ALL THE 8 FEATURES.

COP controllability	COP observability	Distance from the PI
The type of the gate	SCOAP CCO	SCOAP CC1
SCOAP observability	Fanout of the gate	

2) **Procedure for Finding 100 Hard-to-detect Faults in a Circuit:** Traditionally, a 2-stage process is used. First, tests are generated randomly, and then all the common cases are covered. Then the hard-to-detect faults that the first stage could not cover are targeted by a deterministic test generation scheme. This reduces the overall cost of test generation (TG). In line with this philosophy, we run PODEM on 100 hard-to-detect faults (same number used by [5]). Next, we describe the process of finding 100 hard-to-detect faults in a circuit. First, we calculate the COP controllability and observability values of all the nets in the circuit. Then, we calculate the detection probability ( $P_{detect}$ ) of a fault using (2) and (3). We consider a single stuck-at-fault model, which is a logical abstraction of a large number of physical defects (e.g., open, short, etc.) present in a circuit. The detection probability of an s-a-v fault takes into account the probability of activating the fault (given by  $CC(\bar{v})$ ) and the probability of propagating the fault to a PO (given by  $CO(l)$ ).

$$P_{detect} = CC(l) \times CO(l) \text{ for s-a-0 fault at net } l \quad (2)$$

$$P_{detect} = (1 - CC(l)) \times CO(l) \text{ for s-a-1 fault at net } l \quad (3)$$

The fault list is sorted in an ascending order of the detection probability. Finally, we run PODEM on the first 100 faults of the sorted fault list. These faults have the lowest detection probability and hence are the hardest-to-detect (from our point of view).

3) **Output of the Model:** We generated the ground truth label for each circuit net by running PODEM with COP controllability values as a heuristic while backtracing for 100 hard-to-detect faults of the circuit. During the backtracing procedure of PODEM, if a PI assignment does not lead to any conflict, we label the nets involved in the backtrace as ‘1’, else as ‘0’. A circuit net occurs several times during a single run of PODEM. The input features of a circuit net remain the same across its occurrences, but the ground truth label may keep changing. Hence, we computed the probability of no backtrack ( $p$ ) for a circuit net  $l$  as follows:

$$p = \frac{f(label_l = 1)}{f_l} \quad (4)$$

Here,  $f(label_l = 1)$  is the frequency of the occurrence of a ‘1’ in the label for the net  $l$  and  $f_l$  is the frequency with which the net  $l$  appears in the data. The attributes of the model’s output are mentioned in Table IV.

TABLE IV  
THE OUTPUT OF THE LOWER-LEVEL PREDICTOR (ML MODEL) AND ITS ATTRIBUTES

Output Features	Data Type	Size (in bytes)	Range
Probability of no-backtrack	float	4	[0, 1]

### C. Network Architectures

**Hybrid Neural Network (HybNN):** We designed a fully connected feed-forward neural network, which we call *HybNN*. It has two sub-networks: a feature extractor  $E(\theta_f)$  and a regressor  $R(\theta_y)$ . Here,  $\theta_f$  and  $\theta_y$  represent the learnable parameters of the respective sub-networks. The feature extractor takes the features of a circuit net as the inputs and performs further extraction to learn the most significant features. We define a linear layer followed by a nonlinear activation function, *rectified linear unit (ReLU)*, as a hidden layer. Every nonlinear layer adds to the complexity and the learning capability of the network. Hence, deeper networks with more hidden layers are found to perform well [31].  $E(\theta_f)$  has two such hidden layers. The output of the function  $E(\theta_f)$  is fed to the function  $R(\theta_y)$ .  $R(\theta_y)$  consists of a single hidden layer and an output layer followed by a *sigmoid* layer. The output of the regressor network is the no-backtrack probability, which is used as the backtracing heuristic. Each neuron in a layer of *HybNN* is connected to all the neurons in the next layer. The detailed architecture of *HybNN* is shown in Fig. 4. The change in the loss function with respect to the model parameters is given

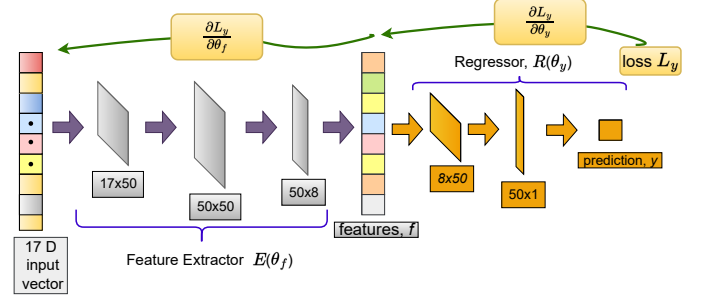


Fig. 4. The architecture of the proposed HybNN model with its sub-networks: feature extractor and regressor.

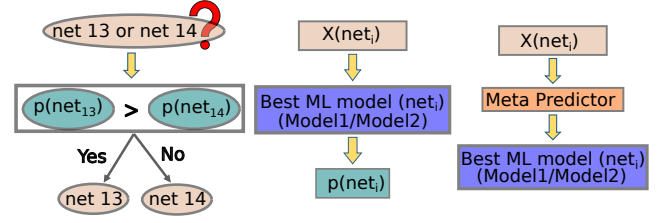


Fig. 5. The concept of the HybMT model.  $X(net_i)$  represents the input features of the  $i^{th}$  net.

by  $\frac{\partial L_y}{\partial \theta_y}$  and  $\frac{\partial L_y}{\partial \theta_f}$  for the regressor and the feature extractor, respectively. These gradient values are propagated backwards to train HybNN as shown in Fig. 4.

**Hybrid Meta Predictor (HybMT):** A meta-predictor model learns to choose among the best predictor models for a given test instance at runtime. We designed a hybrid meta-predictor (called as *HybMT*) model that selects between the two best performing lower-level models. The inputs to the *HybMT* model are the features of a circuit net described in Table III and the output is a class label corresponding to the best-performing model. *HybMT* is a *random forest classifier (RFC)* model designed for a binary classification task. An RFC model is based on an ensemble learning technique. An RFC model combines the predictions of different decision tree classifiers to give a more accurate prediction than its constituent models. We justify the need for the *HybMT* model in Section IV. We get the no-backtrack probability ( $p$ ) for each net from the lower-level model corresponding to the predicted class. Next, we use  $p$  to guide the backtracing step in PODEM. The concept of *HybMT*-based PODEM for the circuit of Fig. 3 is illustrated in Fig. 5.

## IV. EXPERIMENTS AND RESULTS

### A. Basic Setup

We modified an open-source ATPG framework for PODEM obtained from Fault [20], a part of Google’s OpenLane project [32] to incorporate our changes. We used Flex v2.6.4 and Bison v3.0.4 for parsing the net lists in the ISCAS [19] format. We implemented the ANNs using PyTorch v1.10.2 [33]. We



conducted experiments to find the optimal learning rate of the Adam optimizer and set it to 0.01.

The baseline is a faithful implementation of the algorithm described in reference [5]. We have used a *standard setup* for evaluating our scheme [5]. The same setup including the same set of benchmarks have been used in recent papers in the area.

**Data Preparation:** Training and test data points must be entirely different (and disjoint) to ensure the correctness and generalizability of the ML models. Hence, we follow a scheme of leave-one-out testing where we keep one benchmark circuit separate for performing inference and train on the remaining benchmark circuits. We follow this procedure for all the benchmarks.

**Cross-Validation:** We further divide the training set obtained from the leave-one-out scheme into  $k$  equal parts. We keep one of the parts as the validation set, and the other parts constitute the training set. We evaluate the models on the validation set. We repeat this procedure for each data fold. Then, the average accuracy or loss is computed across the  $k$ -folds. As each of the data points is used for validating the model, the cross-validation score shows the model’s generalization capability.

### B. Lower-level Predictors: Experiments and Results

1) *Traditional ML Models:* We started with performing experiments with different regression models: Regularized Linear Regressors (LASSO and Ridge), Support Vector Regressor (SVR), Decision Tree Regressor (DTR) and Random Forest Regressor (RFR) for the no-backtrack probability prediction task. We used 5-fold cross-validation to tune the hyperparameters of these models. The models, their hyperparameters, and the choice of the range of values for tuning are shown in Table V.

TABLE V  
MODELS FOR REGRESSION WITH THEIR HYPERPARAMETERS AND RANGES FOR TUNING

Models	Hyperparameters	Range
Lasso	Regularization coefficient (alpha)	100 values in the range [0.1,1]
Ridge	Regularization coefficient (alpha)	100 values in the range [0.1,1]
SVR	Regularization coefficient (C)	[1e-3, 1e4]
DTR	Depth of the tree	[1,31]
RFR	Number of decision trees	[1,101] in steps of 10

2) *Our Proposed Hybrid Neural Network (HybNN):* The loss function and the optimizer used for training the *HybNN* model are *mean squared error* (MSE) and *Adam*, respectively. We used a uniform distribution in the range  $(-\sqrt{k}, \sqrt{k})$  to initialize the model weights, where  $k = \frac{1}{\text{\#input features}}$ .

3) *Execution Times for the ISCAS’85 Suite:* We ran PODEM on 100 hard-to-detect faults of the benchmark circuits (results shown in Fig. 6). Let us ignore the results for HybMT (last bar in each cluster) for the time being. We observe that the two best-performing models in terms of their highest geometric mean speedups are HybNN and SVR, respectively. *HybNN* shows a reduction of **18.8%** in CPU time as compared to the baseline, and SVR shows a mean reduction of 1.2%. The superior results with our proposed HybNN model compared

to other traditional ML models reinforce the fact that well-designed and highly-tuned neural networks are more expressive and perform feature extraction better than traditional ML models. HybNN learns important features for a net and uses these features to predict the no-backtrack probability at the net. Out of the 10 benchmarks, HybNN is the best performing model in 8/10 and for the remaining two, SVR is the best.

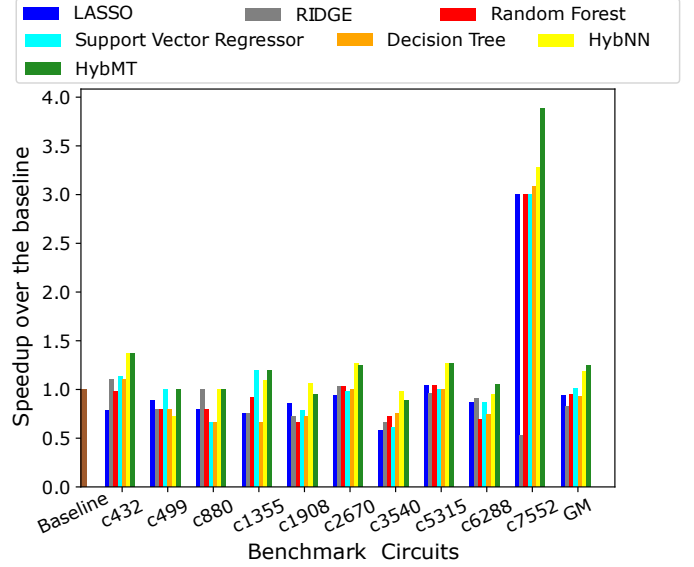


Fig. 6. Speedup obtained over the baseline for 100 hard-to-detect faults (ISCAS’85 suite)

**Motivation for the HybMT model:** These results indicate that there is no unanimous winner among all the ML models that we considered even though HybNN comes close. A hybrid meta-predictor is thus a promising idea as long as it correctly chooses between HybNN and SVR.

### C. HybMT: Training and Results

We generated the ground truth labels for the meta predictor (*HybMT*) model in two ways. In the first approach, we record the number of times a net is backtracked while running PODEM using different ML model-based probabilities as a heuristic. We take the model that gives the minimum number of backtracks for a net as its class label. Recall that by analyzing the CPU time improvements of the lower level regressors, we found that *HybNN* and SVR performed the best for 8 and 2 benchmark circuits, respectively. Hence, in the second approach, we assigned a class label of 0 and 1 to all the nets of the circuits where *HybNN* and SVR perform the best (resp.).

We obtained better results with the second approach – a coarse-grained approach. The results also corroborate the fact that generating the ground truth labels at the circuit level captures a global view of the circuit’s structure and hence gives better results. The *HybMT* meta-predictor (top level) achieves an average 5-fold cross-validation accuracy of 99% for the low-level predictor selection task. The results show that our

proposed *HybMT* model reduces the CPU time of PODEM by **24.4%** over the baseline for the ISCAS'85 benchmark circuits.

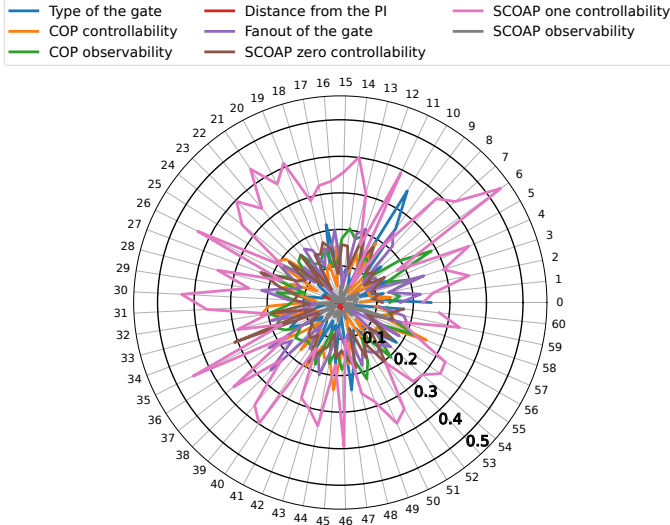


Fig. 7. Importance of the features in the decision trees of the RFC meta predictor model

The radar plot of Fig. 7 shows the importance of each feature in the decision making process of the decision trees of the random forest model (for lower-level predictor selection using *HybMT*). The greater the importance of a feature, the more it is used in making decisions for the data samples. The x-axis represents the decision trees of the *HybMT* model, and the y-axis represents the number of times a feature is used to split a decision tree node, weighted by the number of samples it splits. We observed that *SCOAP one controllability* is the most important feature of all. The results are trying to say that the character of a net is primarily determined by the minimum number of PIs that can control it.

#### D. Experimental Setup of the Commercial ATPG Tool

We ran experiments on a commercial ATPG tool for 100 random faults of the EPFL benchmark circuits. The commercial tool takes scan-inserted netlists as input, which is different from BENCH netlists (input to our *HybMT* algorithm). Hence, it is not possible to obtain the same fault list or even find the hard-to-detect faults for the commercial tool – it does not report such faults separately. So, we ran experiments for faults in the first 100 nets of the scan-inserted netlists and the 100 most hard-to-detect faults in the BENCH netlists (for us). It is important to note that this comparative study is biased against us. *HybMT* runs for the most hard-to-detect faults and still gains performance improvements without losing fault coverage when compared with 100 random faults for the commercial tool.

#### E. *HybMT*: Results on the EPFL Benchmark Circuits

Next, we considered the EPFL benchmark suite [18] (arithmetic circuits), which are much larger. Table VII shows the

absolute CPU time and fault coverage results for the commercial tool, the baseline, and our proposed *HybMT* algorithm. Note that we consider the same fault list for both *HybMT* and baseline. We trained our model on the ISCAS'85 suite (roughly 100 times smaller) and tested it on the EPFL arithmetic suite – there are 10 circuits (in total). Our algorithm had coverage issues with 3 out of the 10, and thus we don't report their results. For the rest 7, our *HybMT* algorithm obtains a speedup of **32.6%** over the commercial tool while obtaining the same fault coverage. We also performed experiments with the baseline [5] on the EPFL circuits and observed a speedup of **95.5%** over the baseline. In terms of coverage, we are roughly neck-and-neck with the baseline. In general, we are better than the commercial tool by roughly 2% (fault coverage), other than one benchmark circuit *Divisor*. This proves that *HybMT* is more efficient and robust than both the commercial tool and the baseline.

We performed extensive experiments to ensure that our fault coverage is the same or better than the commercial ATPG tool for the log2, hypotenuse and square-root circuits of the EPFL benchmark but we were not very successful mainly because these are very large circuits. For example the coverage values for these three benchmarks are 40%, 48% and 6% for *HybMT* (resp.) and they are 90%, 92% and 56% for the commercial tool. We ran these benchmark circuits on Atalanta [34], an ATPG tool based on *fanout-oriented algorithm* (FAN) [21]. Atalanta [34] gives a fault coverage of 79% for the log2 circuit at the cost of 19 times higher CPU time, while failing to generate test patterns for hypotenuse and square-root. As Atalanta performs worse than *HybMT* for the rest of the circuits, we do not include it in our framework. We studied and visualized these circuits and observed that they have large number of gates and dense interconnections. Hence, we see the characterization of these circuits and development of yet more robust learning algorithms as potential future work.

#### V. RELATED WORK

Our primary focus was on recent work (published in the last three years) in the area of ML-based ATPG algorithms that target stuck-at faults. Almost all the highly cited and well regarded work in this field follows the same line of thinking, which is to reduce the number of backtracks in highly optimized versions of PODEM.

In 2020, Roy et al. [35] used the output of ANNs as a backtracing heuristic in PODEM. This was the seminal paper (in recent times). A year later, Roy et al. [5] proposed improvements in the training strategy. In this approach, the backtrace history of a fault is only included in the training data if it decreases the number of backtracks in the ANN-guided PODEM algorithm and the training data is generated by running PODEM on both easy and hard to detect faults of the circuits.

In these works, the ANN used the following input features: distance from the PI (primary input), testability measures and the type of the gate driven by the line. The experiments were performed on 100 hard-to-detect faults of the ISCAS'85 [19]

TABLE VI  
RESULTS OBTAINED FROM THE RE-IMPLEMENTATION OF THE BASELINE [5] AND OUR PROPOSED APPROACH (*HybMT*)

Benchmark Circuits	Baseline (Existing Approach)			<i>HybMT</i> (Proposed Approach)			Fault Coverage <sup>b</sup> (in %)
	CPU Time (in ms)	#Backtraces	#Backtracks	CPU Time (in ms)	#Backtraces	#Backtracks	
c432	410	35,398	15,612	<b>300</b>	31,222	13,730	100
c499	80	6,554	8	<b>80</b>	6,554	8	90
c880	40	1,754	0	<b>40</b>	1,869	0	100
c1355	120	7,435	125	<b>100</b>	6,758	113	100
c1908	180	12,532	3,051	<b>190</b>	14,186	131	100
c2670	2350	2,00,088	98,255	<b>1880</b>	1,81,840	89,136	93
c3540	460	32,933	14,232	<b>520</b>	37,375	16,931	95
c5315	240	6,345	148	<b>190</b>	6,095	393	100
c6288	200	5,600	329	<b>190</b>	4,752	365	80
c7552	1050	89,515	40,272	<b>270</b>	9,424	193	96/100

<sup>b</sup>Except for the benchmark circuit c7552, the fault coverage is the same for both the baseline and the proposed approach.

TABLE VII  
RESULTS OBTAINED FROM A COMMERCIAL TOOL, THE RE-IMPLEMENTATION OF THE BASELINE [5] AND OUR PROPOSED APPROACH (*HybMT*) FOR THE EPFL BENCHMARK CIRCUITS

Benchmark Circuits	CPU Time (in ms)			Fault Coverage (in %)		
	Commercial ATPG Tool	Baseline	<i>HybMT</i>	Commercial ATPG Tool	Baseline	<i>HybMT</i>
Adder	190	2,891	<b>22</b>	98	100	<b>100</b>
Barrel-shifter	340	<b>50</b>	<b>56</b>	98	100	<b>100</b>
Divisor	<b>46,480</b>	46,756	8,05,154	<b>98</b>	97	82
Max	950	44	<b>23</b>	98	100	<b>100</b>
Multiplier	2,510	2,545	<b>1,968</b>	98	100	<b>100</b>
Sine	<b>790</b>	3,25,340	<b>40,850</b>	<b>97</b>	74	<b>97</b>
Square	1,870	<b>647</b>	<b>796</b>	98	98	<b>98</b>

and ITC'99 [36] benchmark circuits. Subsequently, Roy et al. [7] proposed a method based on unsupervised learning to combine different heuristics using *principal component* (PCA) analysis. The major PCs are used for guiding the backtracing in PODEM. This method also uses the testability measures from the Sandia Controllability and Observability Analysis Program (SCOAP) [37] and the fanout count as the input features. PCA-assisted supervised learning has also been explored in [6] to reduce the complexity of the ANN used for guiding the backtracing in PODEM. So far, no work has presented a robust data generation technique or demonstrated consistent improvement across all benchmark circuits. Thus, they highlight a need for a more robust, accurate and better approach.

At the same time, Chowdhury et al. [29] proposed an alternative metric to train and evaluate ML models in the context of IC testing. They also presented an analysis of the state-of-the-art deep learning models' robustness to perturbations. The work showed that ML models' outputs may be poor for regression/classification tasks in ATPG, may be prone to overfitting and may take a prohibitive amount of time for test generation. Our methodology took these pitfalls into account.

In this paper, we compare our work with the latest work in this series that experimentally provided the best results, which is reference [5].

## VI. CONCLUSION

The aim of this paper was to reduce the CPU time of the PODEM algorithm as much as possible without sacrificing the fault coverage for the most *hard-to-detect* faults. Our novel two-level predictor *HybMT* model based PODEM outperforms the existing state-of-the-art algorithm [5] by **24.4%** and **95.5%** for the ISCAS'85 and EPFL benchmarks, respectively. *HybMT* also obtains a speedup of **32.6%** over a commercial tool for the EPFL benchmarks. We used the lower-level models to predict the *no-backtrack probability* ( $p$ ), and then we used  $p$  to guide backtracing in PODEM. We experimented with different traditional ML and neural network models to serve as the lower level models. We found that our novel *HybNN* model and the *support vector regressor* (SVR) models perform the best for different benchmark circuits. Our work shows a significant reduction in the CPU time of PODEM while achieving **high fault coverage** for the ISCAS'85 [19] and EPFL [18] benchmark circuits.

We further conclude that in our work, a global circuit-level view is required to learn better backtracing heuristics. Properly designed neural networks are capable of learning better features and hence are a better candidate for guiding backtracing. The explanations for the meta predictor model indicate that the SCOAP one controllability occurs the maximum number of times in the decision making process of the decision trees



of the random forest classifier and hence is the most important feature.

## REFERENCES

- [1] P. Venkataramani, "Reducing ate test time by voltage and frequency scaling," Ph.D. dissertation, 2014.
- [2] "The race to zero defects in auto ics," 2022. [Online]. Available: <https://semiengineering.com/the-race-to-zero-defects-in-auto-ics>
- [3] "How a chip shortage snarled everything from phones to cars," 2021. [Online]. Available: <https://www.bloomberg.com/graphics/2021-semiconductors-chips-shortage/>
- [4] "Chip-shortage 'crisis' halts car-company output," 2021. [Online]. Available: <https://www.bbc.com/news/technology-55704936>
- [5] S. Roy, S. K. Millican, and V. D. Agrawal, "Training neural network for machine intelligence in automatic test pattern generator," in *2021 34th International Conference on VLSI Design and 2021 20th International Conference on Embedded Systems (VLSID)*. IEEE, 2021, pp. 316–321.
- [6] —, "Principal component analysis in machine intelligence-based test generation," in *2021 IEEE Microelectronics Design & Test Symposium (MDTS)*. IEEE, 2021, pp. 1–6.
- [7] —, "Unsupervised learning in test generation for digital integrated circuits," in *2021 IEEE European Test Symposium (ETS)*. IEEE, 2021, pp. 1–4.
- [8] —, "Special session—machine learning in test: A survey of analog, digital, memory, and rf integrated circuits," in *2021 IEEE 39th VLSI Test Symposium (VTS)*. IEEE, 2021, pp. 1–14.
- [9] Z. Dai, H. Liu, Q. V. Le, and M. Tan, "Coatnet: Marrying convolution and attention for all data sizes," *Advances in Neural Information Processing Systems*, vol. 34, pp. 3965–3977, 2021.
- [10] J. Devlin, M.-W. Chang, K. Lee, and K. Toutanova, "Bert: Pre-training of deep bidirectional transformers for language understanding," *arXiv preprint arXiv:1810.04805*, 2018.
- [11] G. Huang, J. Hu, Y. He, J. Liu, M. Ma, Z. Shen, J. Wu, Y. Xu, H. Zhang, K. Zhong *et al.*, "Machine learning for electronic design automation: A survey," *ACM Transactions on Design Automation of Electronic Systems (TODAES)*, vol. 26, no. 5, pp. 1–46, 2021.
- [12] R. Chen, W. Zhong, H. Yang, H. Geng, F. Yang, X. Zeng, and B. Yu, "Faster region-based hotspot detection," *IEEE Transactions on Computer-Aided Design of Integrated Circuits and Systems*, 2020.
- [13] A. Hosny, S. Hashemi, M. Shalan, and S. Reda, "Drills: Deep reinforcement learning for logic synthesis," in *2020 25th Asia and South Pacific Design Automation Conference (ASP-DAC)*. IEEE, 2020, pp. 581–586.
- [14] H. Zhou, W. Jin, and S. X.-D. Tan, "Gridnet: Fast data-driven em-induced ir drop prediction and localized fixing for on-chip power grid networks," in *2020 IEEE/ACM International Conference On Computer Aided Design (ICCAD)*. IEEE, 2020, pp. 1–9.
- [15] J. Chen, J. Kuang, G. Zhao, D. J.-H. Huang, and E. F. Young, "Pros: A plug-in for routability optimization applied in the state-of-the-art commercial eda tool using deep learning," in *2020 IEEE/ACM International Conference On Computer Aided Design (ICCAD)*. IEEE, 2020, pp. 1–8.
- [16] H. Dhotre, S. Eggersgluß, M. Dehbashi, U. Pfannkuchen, and R. Drechsler, "Machine learning based test pattern analysis for localizing critical power activity areas," in *2017 IEEE International Symposium on Defect and Fault Tolerance in VLSI and Nanotechnology Systems (DFT)*. IEEE, 2017, pp. 1–6.
- [17] S. N. Mozaffari, B. Bhaskaran, K. Narayanun, A. Abdollahian, V. Pagalone, S. Sarangi, and J. E. Colburn, "An efficient supervised learning method to predict power supply noise during at-speed test," in *2019 IEEE International Test Conference (ITC)*. IEEE, 2019, pp. 1–10.
- [18] L. Amarú, P.-E. Gaillardon, and G. De Micheli, "The epfl combinational benchmark suite," in *Proceedings of the 24th International Workshop on Logic & Synthesis (IWLS)*, no. CONF, 2015.
- [19] F. Brglez, "A neutral netlist of 10 combinatorial benchmark circuits and a target translator in fortran," in *Int. Symposium on Circuits and Systems, Special Session on ATPG and Fault Simulation, June 1985*, 1985, pp. 663–698.
- [20] M. Abdelatty, M. Gaber, and M. Shalan, "Fault: Open-source eda's missing dft toolchain," *IEEE Design & Test*, vol. 38, no. 2, pp. 45–52, 2021.
- [21] H. Fujiwara and T. Shimono, "On the acceleration of test generation algorithms," *IEEE Transactions on Computers*, vol. 32, no. 12, pp. 1137–1144, 1983.
- [22] P. Goel, "An implicit enumeration algorithm to generate tests for combinational logic circuits," *IEEE transactions on Computers*, vol. 30, no. 03, pp. 215–222, 1981.
- [23] M. Abramovici, M. A. Breuer, A. D. Friedman *et al.*, *Digital systems testing and testable design*. Computer science press New York, 1990, vol. 2.
- [24] M. Bushnell and V. Agrawal, *Essentials of electronic testing for digital, memory and mixed-signal VLSI circuits*. Springer Science & Business Media, 2004, vol. 17.
- [25] F. Brglez, "On testability analysis of combinational circuits," in *Proc. International Symp. Circuits and Systems*, 1984, pp. 221–225.
- [26] L. Goldstein, "Controllability/observability analysis of digital circuits," *IEEE Transactions on Circuits and Systems*, vol. 26, no. 9, pp. 685–693, 1979.
- [27] M. N. Mondal, A. B. Chowdhury, M. Pradhan, S. Sur-Kolay, and B. B. Bhattacharya, "Fault coverage of a test set on structure-preserving siblings of a circuit-under-test," in *2019 IEEE 28th Asian Test Symposium (ATS)*. IEEE, 2019, pp. 25–255.
- [28] Z. Shi, M. Li, S. Khan, L. Wang, N. Wang, Y. Huang, and Q. Xu, "Deeptpi: Test point insertion with deep reinforcement learning," in *2022 IEEE International Test Conference (ITC)*. IEEE, 2022, pp. 194–203.
- [29] A. B. Chowdhury, B. Tan, S. Garg, and R. Karri, "Robust deep learning for ic test problems," *IEEE Transactions on Computer-Aided Design of Integrated Circuits and Systems*, vol. 41, no. 1, pp. 183–195, 2021.
- [30] R. Brayton and A. Mishchenko, "Abc: An academic industrial-strength verification tool," in *Computer Aided Verification: 22nd International Conference, CAV 2010, Edinburgh, UK, July 15-19, 2010. Proceedings* 22. Springer, 2010, pp. 24–40.
- [31] G. F. Montufar, R. Pascanu, K. Cho, and Y. Bengio, "On the number of linear regions of deep neural networks," *Advances in neural information processing systems*, vol. 27, 2014.
- [32] A. Ghazy and M. Shalan, "Openlane: The open-source digital asic implementation flow," in *Proc. Workshop on Open-Source EDA Technol.(WOSET)*, 2020.
- [33] A. Paszke, S. Gross, F. Massa, A. Lerer, J. Bradbury, G. Chanan, T. Killeen, Z. Lin, N. Gimelshein, L. Antiga *et al.*, "Pytorch: An imperative style, high-performance deep learning library," *Advances in neural information processing systems*, vol. 32, 2019.
- [34] H. Lee and D. S. Ha, "On the generation of test patterns for combinational circuits," Technical Report, Tech. Rep., 1993.
- [35] S. Roy, S. K. Millican, and V. D. Agrawal, "Machine intelligence for efficient test pattern generation," in *2020 IEEE International Test Conference (ITC)*. IEEE, 2020, pp. 1–5.
- [36] F. Corno, M. S. Reorda, and G. Squillero, "Rt-level itc'99 benchmarks and first atpg results," *IEEE Design & Test of computers*, vol. 17, no. 3, pp. 44–53, 2000.
- [37] L. H. Goldstein and E. L. Thigpen, "Scoop: Sandia controllability/observability analysis program," in *Proceedings of the 17th Design Automation Conference*, 1980, pp. 190–196.